JOURNAL OF COMPUTATIONAL PHYSICS 107, 213–224 (1993)

Spectral Multigrid Methods for the Reformulated Stokes Equations

WILHELM HEINRICHS

Mathematisches Institut der Heinrich-Heine-Universität Düsseldorf, Universitätsstraße 1, D-4000 Düsseldorf 1, Germany

Received March 4, 1991; revised March 26, 1992

We present a spectral multigrid method for the reformulated Stokes equations. Here the continuity equation is replaced by a Poisson equation for the pressure. This system is discretized by a spectral collocation method without introducing a staggered grid. We observed no spurious modes except the physical one which is identical to a constant. Hence no filtering techniques are needed. We present an effective finite difference preconditioner which is employed for relaxation inside of the spectral multigrid method. Numerical results are presented which show the efficiency of our method.

1. INTRODUCTION

We consider a reformulation of the Stokes equations where the continuity equation is replaced by a Poisson-like equation for the pressure. To guarantee full equivalence between the two systems of equations (provided all functions are sufficiently smooth) the continuity equation has to hold at the boundary of the domain. This treatment has been proposed in the famous article of Harlow and Welch [13]. They proposed the MAC method which obtains an equation containing Δp (p denotes the pressure) by differentiating the time-dependent momentum equations and adding them. For finite difference discretizations this approach turned out to be very useful for the efficient solution with multigrid techniques (see [31, 24]). Furthermore, it is not difficult to parallelize and vectorize this algorithm. For more information on parallel multigrid solvers for the Navier–Stokes equations on general 2D domains we refer to [25].

We were interested in the performance of spectral multigrid methods for the reformulated Navier–Stokes equations. Here the spectral discretization is accomplished by a pseudospectral (or collocation) method using Chebyshev polynomials. The collocation points are given by the standard Chebyshev Gauss–Lobatto nodes. In particular, we introduce a Chebyshev collocation method which has the following desirable properties:

- high spectral accuracy,
- no spurious modes except the physical one (constant solution),
- no staggered grids.

If the continuity equation is directly discretized by a spectral method, the pressure is affected by spurious modes (seven modes) which deteriorate the accuracy of the method. By our spectral discretization of the reformulated Stokes equations spurious modes (except the constant) are avoided. A similar approach was already introduced by Kleiser and Schumann [23], where the parasite modes are implicitly filtered out by the solution process. Quite good survey about the occurrence of spurious modes for spectral discretizations of the Navier–Stokes equations is given in [1; 6, Chap. 11.3].

In our method the spurious pressure modes are ruled out by enforcing a Poisson equation on the pressure rather than the usual divergence-free condition (three spurious modes) and the x-component of the momentum equation at the four corners (the remaining four spurious modes). This result is proven in Theorem 3.1. In our method the divergence-free condition is treated implicitly. This treatment is recommended for rectangular domains. For more complex domains (already for trapezoidal domains) it cannot be extended in a straightforward manner. Here one has to use a domain decomposition approach, where the complex domain is partitioned in a number of rectangular subdomains. An explicit treatment of the boundary equations also works for more complex domains but preconditioning by finite differences is quite poor. The eigenvalues of the preconditioned spectral operator are complex and the imaginary parts are quite large. A simple Richardson iteration with fixed relaxation parameters does not converge. Here we recommend the use of nonsymmetric matrix iterations. For instance, the GMRES iteration (see [29, 30]) is

0021-9991/93 $5.00

quite a good choice. For our implicit method we use a velocity field which is two degrees higher in the space variable, where the Neumann boundary condition has to be enforced. The advantage of this choice is due to the fact that fast Fourier transforms (FFTs) are now available. This makes the method very efficient. If the velocity field would be of the same degree N in each variable, then the complementary factor for the pressure would be $N-2$, for which FFT could not be used.

Furthermore, it is well known (see, e.g., [2]) that spurious modes can also be avoided by introducing staggered grids. In [2] the continuity equation is discretized by using the Gauss points instead of the Gauss–Lobatto points. However, this approach is quite expensive in numerical computations since one has to interpolate between these two meshes.

We also present an efficient finite difference preconditioner for the spectral system. The eigenvalues of the preconditioned spectral operator are complex and lie in a circle C which intersects the real axes in the points one and $\pi^2/4$. These eigenvalue bounds are already well known from similar considerations for the Poisson equation. Due to the good performance of finite difference preconditioning techniques we prefer a preconditioned Richardson relaxation for the iterative solution of the spectral systems. Finally, we show the efficiency of a spectral multigrid method which employs the standard multigrid components (see [14, 15, 32, 33]).

The proposed method is one of the few existing spectral methods of "global" type; i.e., it does not reduce a Stokes problem to a sequence of Poisson type problems which results from the Uzawa decoupling procedure. The decoupling in a cascade of Poisson problems was originally proposed by Maday, Patera, and Ronquist (see [2, 28]). In the spectral element multigrid method of Patera and Ronquist the Uzawa decoupling procedure leads to an equation for the pressure. The corresponding spectral operator is very well conditioned and this system can easily be solved by a conjugate gradient method in a few steps. In each step one has to solve a Poisson problem. However, our treatment avoids the explicit solution of Poisson problems. Furthermore, our technique can be extended to nonlinear problems resulting from the Navier–Stokes equations. Here our future research deals with finding good preconditioners for an increasing Reynolds number.

In Section 2 we give the reformulated Stokes and Navier–Stokes equations. Then we present in Section 3 the spectral discretization. Here we prove that the spectral schemes have no spurious modes except the physical one. Afterwards we introduce an effective finite difference preconditioner (see Section 4) which is used in the relaxation scheme of the spectral multigrid method (Section 5). Numerical results show the usefulness of our spectral multigrid method.

2. REFORMULATION OF THE NAVIER–STOKES EQUATIONS

We first consider the steady Stokes equations

$$-\Delta u + p_x = f^u \quad \text{in} \quad \Omega = (-1, 1)^2, \tag{2.1}$$

$$-\Delta v + p_y = f^v \quad \text{in } \Omega, \tag{2.2}$$

$$u_x + v_y = 0 \quad \text{in} \quad \bar{\Omega} = [-1, 1]^2 \tag{2.3}$$

with Dirichlet boundary conditions for the velocity field:

$$u = u_0, \qquad v = v_0 \qquad \text{on } \partial\Omega.$$

Here f^u, f^v denote given functions defined in Ω. Since the pressure is only determined up to a constant, we impose the average pressure to be zero, i.e., $\int_\Omega p\, dx = 0$.

Equations (2.1), (2.2) are called the momentum equations and Eq. (2.3) is called the continuity equation. As already mentioned in the Introduction, many difficulties in the numerical solution of the system (2.1)–(2.3) are caused by the special form of the continuity equation, where no Δp occurs. There are several well-known approaches to overcome this problem (see Roache [27, Chap. III-G]).

One way to introduce Δp is described in the famous article of Harlow and Welch [13]. They propose the MAC method which obtains an equation containing Δp by differentiating the time-dependent momentum equations and adding them. Continuity on every new time level is guaranteed by solving this equation with an appropriate right-hand side. Here the continuity equation has to be valid on the boundary, too. This method has been generalized to other time dependent problems by Hirt and Harlow [22].

In the following theorem we derive a new system which is equivalent to (2.1)–(2.3) and which is more appropriate for iterative solvers.

THEOREM 2.1. *Let $u, v \in C^3(\Omega) \cap C^1(\bar{\Omega})$, $p \in C^2(\Omega)$, $f^u, f^v \in C^1(\Omega)$. Then the Stokes system* (2.1)–(2.3) *is equivalent to the following modified system:*

$$-\Delta u + p_x = f^u \qquad \text{in } \Omega, \tag{2.4}$$

$$-\Delta v + p_y = f^v \qquad \text{in } \Omega, \tag{2.5}$$

$$\Delta p = f^u_x + f^v_y \qquad \text{in } \Omega, \tag{2.6}$$

$$u_x + v_y = 0 \qquad \text{on } \partial\Omega. \tag{2.7}$$

Proof. The sum of the derivatives of Eq. (2.1) with respect to x and (2.2) with respect to y yields (2.6). Here we make use of the fact that due to (2.3)

$$-\Delta(u_x + v_y) = 0 \qquad \text{in } \bar{\Omega}. \tag{2.8}$$

In the other direction, Eq. (2.3) can be regained from

Eqs. (2.4)–(2.7) because the difference of the sum of the derivatives of Eqs. (2.4) with respect to x and (2.5) with respect to y and Eq. (2.6) yields Eq. (2.8) and this partial differential equation with the homogeneous Dirichlet boundary conditions (2.7) interpreted as a boundary value problem for $u_x + v_y$ has the unique solution (2.3). ∎

This result can easily be generalized to the Navier–Stokes equations. By Re we denote the Reynolds number.

THEOREM 2.2. *Let* $u,\ v \in C^3(\Omega) \cap C^1(\bar{\Omega})$, $p \in C^2(\Omega)$, $f^u, f^v \in C^1(\Omega)$. *Then the two Navier–Stokes systems,*

$$-\Delta u + \mathrm{Re}(uu_x + vu_y) + p_x = f^u \quad \text{in } \Omega, \tag{2.9}$$

$$-\Delta v + \mathrm{Re}(uv_x + vv_y) + p_y = f^v \quad \text{in } \Omega, \tag{2.10}$$

$$u_x + v_y = 0 \quad \text{in } \bar{\Omega} \tag{2.11}$$

and

$$-\Delta u + \mathrm{Re}(vu_y - uv_y) + p_x = f^u \quad \text{in } \Omega, \tag{2.12}$$

$$-\Delta v + \mathrm{Re}(uv_x - vu_x) + p_y = f^v \quad \text{in } \Omega, \tag{2.13}$$

$$\Delta p + 2\,\mathrm{Re}(v_x u_y - u_x v_y) = f^u_x + f^v_y \quad \text{in } \Omega, \tag{2.14}$$

$$u_x + v_y = 0 \quad \text{on } \partial\Omega \tag{2.15}$$

are fully equivalent.

Proof. Because of (2.11) the momentum equations (2.9)–(2.10) can be written as (2.12)–(2.13). Differentiating (2.12) with respect to x and (2.13) with respect to y, adding these equations, and using the continuity equation (2.11) yields (2.14). In the other direction, the continuity equation can be derived from Eqs. (2.12)–(2.15) by the same argument as in the Stokes case. ∎

For the new Stokes or Navier–Stokes systems we have three boundary conditions for the velocity components but no condition for the pressure. A similar problem also occurred for the biharmonic equation

$$\Delta^2 u = f \quad \text{in } \Omega,$$

$$u = u_n = 0 \quad \text{on } \partial\Omega,$$

where n denotes the outer normal derivative. In [18, 19] we proposed a splitting into a second-order system

$$\Delta v = f \quad \text{in } \Omega, \tag{2.16}$$

$$\Delta u - v = 0 \quad \text{in } \bar{\Omega}, \tag{2.17}$$

where v denotes an auxiliary function defined in $\bar{\Omega}$. Obviously, this system has two boundary conditions for u but not one for v. In [18, 19] we describe a spectral discretization of the system (2.16), (2.17), which allows the efficient use of spectral multigrid techniques. Here we utilize the experience made in these papers in order to derive a suitable spectral multigrid method.

3. SPECTRAL DISCRETIZATION

In order to present the spectral discretization of the reformulated Stokes equations (2.4)–(2.7) we first give some notations. For $N \in \mathbf{N}$ we introduce the following polynomial subspaces:

$$\mathbf{P}_N = \{\text{polynomials of degree less or equal } N \text{ in } x, y\},$$

$$\mathbf{P}^0_{N+2,N} = \{(1-x^2)^2\,(1-y^2)\,p_{N-2} : p_{N-2} \in \mathbf{P}_{N-2}\},$$

$$\mathbf{P}^0_{N,N+2} = \{(1-x^2)(1-y^2)^2\,p_{N-2} : p_{N-2} \in \mathbf{P}_{N-2}\},$$

$$\mathbf{P}^0_N = \{(1-x^2)(1-y^2)\,p_{N-2} : p_{N-2} \in \mathbf{P}_{N-2}\}.$$

Hence the polynomials $p \in \mathbf{P}^0_{N+2,N}$ fulfill $p = p_x = 0$ for $x = \pm 1$, $p = 0$ for $y = \pm 1$, and the polynomials $p \in \mathbf{P}^0_{N,N+2}$ fulfill $p = p_y = 0$ for $y = \pm 1$, $p = 0$ for $x = \pm 1$. The collocation points are given by the standard Chebyshev Gauss–Lobatto nodes:

$$(x_i, y_j) = \left(\cos\frac{i\pi}{N}, \cos\frac{j\pi}{N}\right), \qquad i, j = 0, \ldots, N.$$

Furthermore, we introduce the following collocation grids:

$$\bar{\Omega}_N = \{(x_i, y_j) : i, j = 0, \ldots, N\},$$

$$\Omega_N = \bar{\Omega}_N \cap \Omega,$$

$$\partial\Omega_N = \bar{\Omega}_N \cap \partial\Omega,$$

$$\Omega^{co}_N = \{(1, 1), (-1, 1), (1, -1), (-1, -1)\},$$

$$\Omega^u_N = \{(x_i, y_j) : i = 0, \ldots, N, j = 1, \ldots, N-1\} \cup \Omega^{co}_N,$$

$$\Omega^v_N = \{(x_i, y_j) : i = 1, \ldots, N-1, j = 0, \ldots, N\},$$

$$\Omega^c_N = \Omega_N \cup \Omega^{co}_N,$$

$$\partial\Omega^c_N = \partial\Omega_N - \Omega^{co}_N.$$

Now the pseudospectral (or collocation) discretization of the reformulated Stokes system (2.4)–(2.7) associated with homogeneous Dirichlet boundary conditions (i.e., $u_0 = v_0 = 0$) reads as follows: Find $u_{N+2,N} \in \mathbf{P}^0_{N+2,N}$, $v_{N,N+2} \in \mathbf{P}^0_{N,N+2}$, $p_N \in \mathbf{P}_N$, such that

$$-\Delta u_{N+2,N} + p_{N,x} = f^u \quad \text{in } \Omega^u_N, \tag{3.1}$$

$$-\Delta v_{N,N+2} + p_{N,y} = f^v \quad \text{in } \Omega^v_N, \tag{3.2}$$

$$\Delta p_N = f^u_x + f^v_y \quad \text{in } \Omega_N. \tag{3.3}$$

In (3.1)–(3.3) we choose an implicit treatment of the boundary conditions. Since $u=v=0$ on $\partial\Omega$ we obtain from (2.7) $u_x=0$ along the axes $x=\pm 1$ and $v_y=0$ along the axes $y=\pm 1$. This means that we have two boundary conditions for u in $x=\pm 1$ and two boundary conditions for v in $y=\pm 1$. We approximate u, v by polynomials $u_{N+2,N}\in \mathbf{P}^0_{N+2,N}$, $v_{N,N+2}\in \mathbf{P}^0_{N,N+2}$, which have two more degrees of freedom in the direction where two boundary conditions have to be enforced. A similar treatment was already successfully employed in [18, 19]. Since the boundary conditions are treated implicitly we have to give collocation conditions on the momentum equations in u for $x=\pm 1$ and v for $y=\pm 1$. Furthermore, the boundary conditions $u_x+v_y=0$ in the corners are automatically fulfilled if $u=v=0$ on $\partial\Omega$. Hence these four conditions have to be replaced by four conditions belonging to the momentum equations. Here we impose that (2.4) also holds in the four corners of the domain. Since $\Delta u=0$ in the four corners we obtain the four additional conditions:

$$p_{N,x}=f^u \qquad \text{in the corners.}$$

These conditions are enclosed in Eqs. (3.1) which have to be valid in Ω^u_N. The system (3.1)–(3.3) requires

$$M=2(N-1)^2+(N+1)^2=3N^2-2N+3$$

conditions of collocation for the M unknown coefficients of $u_{N+2,N}$, $v_{N,N+2}$, p_N. Clearly, p_N is only determined up to a constant and has to be normalized such that $\int_\Omega p_N\,dx=0$.

A viable alternative to the above implicit scheme is given by the following explicit method: Find $u_N\in \mathbf{P}^0_N$, $v_N\in \mathbf{P}^0_N$, $p_N\in \mathbf{P}_N$, such that

$$-\Delta u_N+p_{N,x}=f^u \qquad \text{in } \Omega^c_N, \tag{3.4}$$

$$-\Delta v_N+p_{N,y}=f^v \qquad \text{in } \Omega_N, \tag{3.5}$$

$$\Delta p_N=f^u_x+f^v_y \qquad \text{in } \Omega_N, \tag{3.6}$$

$$u_{N,x}+v_{N,y}=0 \qquad \text{on } \partial\Omega^c_N. \tag{3.7}$$

Once more for polynomials u_N, $v_N\in \mathbf{P}^0_N$ the continuity equation is automatically fulfilled in the four corners. Hence we replace these conditions by the four momentum equations.

The system (3.4)–(3.7) yields M conditions of collocation for the M unknowns. Now there is no boundary collocation for the momentum equations. However, a viable disadvantage of this scheme is due to the fact that it does not offer two more degrees of freedom for u in x and v in y. In the numerical experiments it turned out to be somewhat less accurate than the implicit scheme (see also the numerical examples in [19]).

In the case of inhomogeneous Dirichlet boundary conditions we introduce boundary interpolants u^1_N, $v^1_N\in \mathbf{P}_N$ such that

$$u^1_N=u_0 \qquad \text{on } \partial\Omega_N,$$

$$v^1_N=v_0 \qquad \text{on } \partial\Omega_N,$$

$$u^1_{N,x}+v^1_{N,y}=0 \qquad \text{on } \partial\Omega_N.$$

Then one solves the spectral systems with homogeneous Dirichlet boundary conditions, where f^u (resp. f^v) are replaced by $f^u+\Delta u^1_N$ (resp. $f^v+\Delta v^1_N$). This treatment was successfully applied to the driven cavity flow problem in Section 6.

A well-known problem for spectral methods applied to the Stokes equation results from the occurrence of certain "spurious modes" or "parasite modes" for the pressure. They are given by those non-trivial polynomials $q_N\in \mathbf{P}_N$ which yield zero for all collocation conditions. For the implicit scheme (3.1)–(3.3) the spurious modes are characterized by

$$q_{N,x}=0 \qquad \text{in } \Omega^u_N,$$

$$q_{N,y}=0 \qquad \text{in } \Omega^v_N,$$

$$\Delta q_N=0 \qquad \text{in } \Omega_N.$$

For the explicit scheme they are characterized by the equations:

$$q_{N,x}=0 \qquad \text{in } \Omega^c_N,$$

$$q_{N,y}=0 \qquad \text{in } \Omega_N,$$

$$\Delta q_N=0 \qquad \text{in } \Omega_N.$$

Clearly, the physical solution $q\equiv$ const. is one of the spurious modes. From the analysis in [1] it followed that for the standard Chebyshev collocation method the spurious modes are given by the eight functions

$$1,\quad T_N(x),\quad T_N(y),\quad T_N(x)\,T_N(y),$$

$$T'_N(x)\,T'_N(y),\quad xT'_N(x)\,T'_N(y),$$

$$T'_N(x)\,yT'_N(y),\quad xT'_N(x)\,yT'_N(y),$$

where T_N denotes the Nth Chebyshev polynomial. These were the only non-trivial solutions $q_N\in \mathbf{P}_N$ of

$$q_{N,x}=0 \qquad \text{in } \Omega_N,$$

$$q_{N,y}=0 \qquad \text{in } \Omega_N.$$

Since our discretizations require additional collocation conditions the set of spurious modes must be a subset of the above spurious modes. Here we prove that both

discretizations do not introduce other spurious modes than the physical one.

THEOREM 3.1. *The spectral schemes* (3.1)–(3.3) *and* (3.4)–(3.7) *have no spurious modes other than the physical one.*

Proof. The proof is performed for even N. A similar proof can be accomplished for odd N. From the above considerations it is clear that any spurious mode q_N can be written as

$$q_N = q_N^1 + q_N^2,$$

where

$$q_N^1 = \alpha + \beta T_N(x) + \gamma T_N(y) + \delta T_N(x)\, T_N(y),$$
$$q_N^2 = aT_N'(x)\, T_N'(y) + bxT_N'(x)\, T_N'(y) + cT_N'(x)\, yT_N'(y) + dx\, T_N'(x)\, yT_N'(y)$$

and $\alpha, \beta, \gamma, \delta, a, b, c, d \in \mathbf{R}$.

Since both schemes require $\Delta q_N = 0$ in Ω_N and q_N^2 always satisfies $\Delta q_N^2 = 0$ in Ω_N, we finally obtain the conditions $\Delta q_N^1 = 0$ in Ω_N, i.e.,

$$T_N''(x_i)\beta + T_N''(y_j)\gamma + (T_N''(x_i)\, T_N(y_j) + T_N(x_i)\, T_N''(y_j))\,\delta = 0, \qquad i,j = 1, \ldots, N-1.$$

By using the relations

$$T_N''(x_i) = \frac{N^2(-1)^{i+1}}{1-x_i^2}, \qquad i = 1, \ldots, N-1,$$

we further derive

$$\frac{(-1)^i}{\sin^2(i\pi/N)}\beta + \frac{(-1)^j}{\sin^2(j\pi/N)}\gamma + \left(\frac{1}{\sin^2(i\pi/N)} + \frac{1}{\sin^2(j\pi/N)}\right) \times (-1)^{i+j}\delta = 0, \qquad i,j = 1, \ldots, N-1.$$

We now consider the 3×3 system which results by choosing

$$(i,j) \in \left\{\left(\frac{N}{2}, \frac{N}{2}\right), \left(1, \frac{N}{2}\right), \left(\frac{N}{2}, 1\right)\right\}.$$

A simple calculation shows that this system is regular. Its determinant is given by $4(1 + 1/\sin^2(\pi/N)) \neq 0$. Hence we obtain $\beta = \gamma = \delta = 0$. For the remaining modes we consider the four conditions in the corners. Here we require $q_{N,x} = 0$. By using that

$$T_N'(\pm 1) = \pm N^2, \qquad T_N''(\pm 1) = \tfrac{1}{3}N^2(N^2-1),$$
$$(xT_N')'(\pm 1) = \pm \tfrac{1}{3}N^2(N^2+2)$$

and introducing

$$\tilde{a} = \tfrac{1}{3}N^4(N^2-1)a, \qquad \tilde{b} = \tfrac{1}{3}N^4(N^2+2)b,$$
$$\tilde{c} = \tfrac{1}{3}N^4(N^2-1)c, \qquad \tilde{d} = \tfrac{1}{3}N^4(N^2+2)d,$$

we obtain the 4×4 system

$$\begin{bmatrix} 1 & 1 & 1 & 1 \\ 1 & -1 & 1 & -1 \\ -1 & -1 & 1 & 1 \\ -1 & 1 & 1 & -1 \end{bmatrix} \begin{bmatrix} \tilde{a} \\ \tilde{b} \\ \tilde{c} \\ \tilde{d} \end{bmatrix} = 0.$$

The determinant of this system is equal to 16. Hence it is regular and we obtain $a = b = c = d = 0$. Therefore the remaining spurious mode is identical to the constant α. This concludes the proof. ∎

4. PRECONDITIONING

Since the spectral operator has a very large condition number growing as $O(N^4)$ we present an effective finite difference (FD) preconditioner. For the Laplace operator it is well known (see [6, 14, 15, 32, 33]) that the preconditioned spectral operator has real, positive eigenvalues lying in the interval $[1, \pi^2/4]$. This can still be improved by using bilinear finite element preconditioning. Here the eigenvalues are confined to the interval $[0.693, 1]$ (see [7, 8]). In this paper we consider FD preconditioning.

Since the Stokes system contains first-order derivatives we may no more expect that the eigenvalues of the preconditioned spectral Stokes operator are real. But we tried to find a FD preconditioner, where the real parts of the eigenvalues lie in the interval $[1, \pi^2/4]$ and the imaginary parts are relatively small. Now let us describe the FD operator more precisely. Here we give the components in the one-dimensional case. The two-dimensional components can easily be derived by using tensor product representation. For both the velocity components and the pressure we approximate the derivatives as follows (w denotes a one-dimensional function):

$$w''(x_j) \cong a_j w(x_{j-1}) - (a_j + c_j)\, w(x_j) + c_j w(x_{j+1}), \qquad j = 1, \ldots, N-1,$$

where

$$a_j = \frac{\alpha}{s_j s_{j-1/2}}, \qquad c_j = \frac{\alpha}{s_j s_{j+1/2}}$$

and

$$\alpha = \frac{1}{2s_{1/2}s_1}, \quad s_j = \sin\frac{j\pi}{N}, \quad s_{j\pm 1/2} = \sin\frac{(j\pm 1/2)\pi}{N}$$

$$w''(x_0) \cong \frac{1}{2s_{1/2}^4}(w(x_1) - w(x_0)),$$

$$w''(x_N) \cong \frac{1}{2s_{1/2}^4}(w(x_{N-1}) - w(x_N)),$$

$$w'(x_0) \cong \frac{1}{2s_{1/2}^2}(w(x_0) - w(x_1)),$$

$$w'(x_N) \cong \frac{1}{2s_{1/2}^2}(w(x_{N-1}) - w(x_N)).$$

For the second derivative we employed standard central differences with respect to the Chebyshev mesh. In the boundary points we introduced outer points which were eliminated by using the Neumann boundary conditions (for the velocity components). The first derivatives in boundary points are approximated by one-sided finite differences. Now we consider the spectral system (3.1)–(3.3), where the continuity equation is treated implicitly. The corresponding spectral (resp. FD) operators are written as

$$L_{sp}^{im} \in \mathbf{R}^{M,M} \qquad (\text{resp. } L_{FD}^{im} \in \mathbf{R}^{M,M}).$$

Clearly, the eigenvalues of L_{sp}^{im}, L_{FD}^{im} are complex where the absolute value increases as $O(N^4)$. One eigenvalue is zero due to the presence of one spurious mode which is identical to the constant. In order to obtain regular operators we considered the operators which are obtained by eliminating the last column and row of the system. In the following tables we present the (absolutely) minimal and maximal eigenvalues λ_{min} and λ_{max} of the preconditioned operators:

$$\lambda_{min} = \min\{|\lambda| : \lambda \text{ eigenvalue of } (L_{FD}^{im})^{-1} L_{sp}^{im}\},$$

$$\lambda_{max} = \max\{|\lambda| : \lambda \text{ eigenvalue of } (L_{FD}^{im})^{-1} L_{sp}^{im}\}.$$

In Table I we present λ_{min}, λ_{max} for $N = 4, 8, 12$.

The eigenvalues belonging to λ_{min} and λ_{max} are real. Hence the absolute values of the eigenvalues lie in the interval $[1, \pi^2/4]$. In Figs. 1 and 2 we plotted the eigenvalues for

TABLE I

λ_{min}, λ_{max} of $(L_{FD}^{im})^{-1} L_{sp}^{im}$

N	λ_{min}	λ_{max}
4	1.00	2.4284
8	1.00	2.3867
12	1.00	2.4231

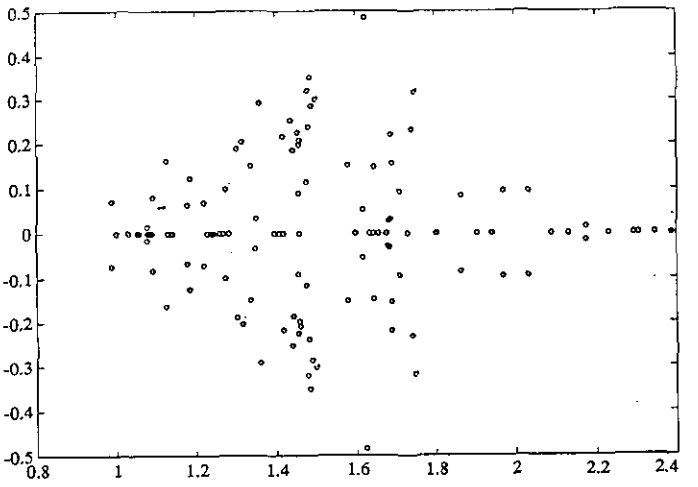

FIG. 1. Eigenvalues of $(L_{FD}^{im})^{-1} L_{sp}^{im}$ for $N = 8$.

$N = 8$ and $N = 12$. It can be seen that the imaginary parts are relatively small, always less than 0.5. The eigenvalues with the largest imaginary parts lie in the "middle" of the eigenvalue spectrum with a real part of about 1.6–1.7. From the figures it can be seen that almost all eigenvalues lie in the circle C given by

$$C = \left\{(\rho, \sigma) : \left(\rho - \frac{1}{2}\left(1 + \frac{\pi^2}{4}\right)\right)^2 + \sigma^2 \leqslant \frac{1}{4}\left(\frac{\pi^2}{4} - 1\right)^2\right\}.$$

Only the complex eigenvalue with smallest real part (about 0.99) is a little bit outside of C. But this will not disturb the convergence if we choose the relaxation parameters based on C. For a Richardson relaxation (see [14, 15]), we therefore choose the relaxation parameter ω equal to

$$\omega = \frac{2}{1 + \pi^2/4}.$$

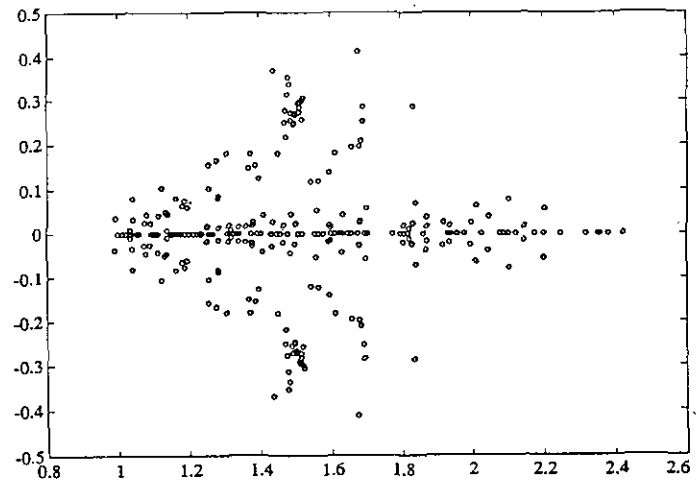

FIG. 2. Eigenvalues of $(L_{FD}^{im})^{-1} L_{sp}^{im}$ for $N = 12$.

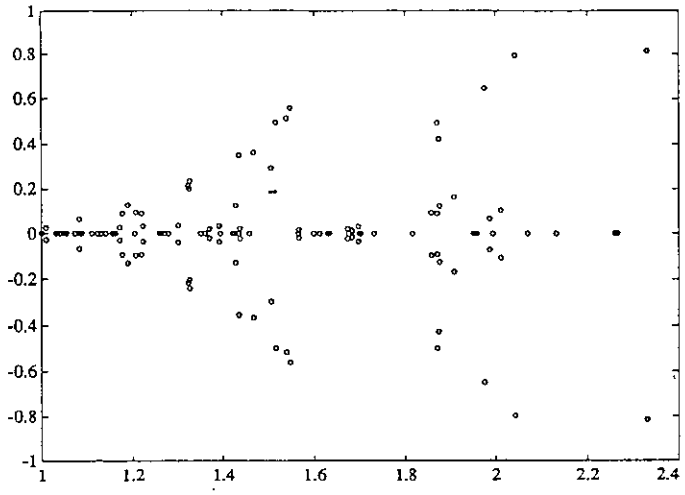

FIG. 3. Eigenvalues of $(L_{FD}^{ex})^{-1} L_{sp}^{ex}$ for $N = 8$.

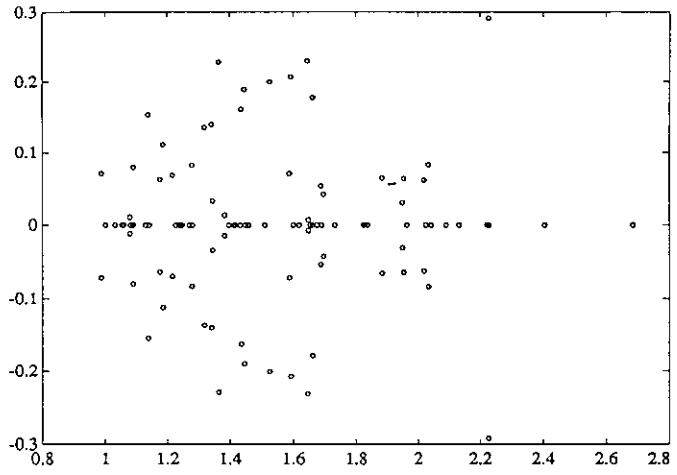

FIG. 5. Eigenvalues of $(L_{FD,sp}^{ex})^{-1} L_{sp}^{ex}$ for $N = 8$.

Then the Richardson iteration matrix has a spectral radius ρ of

$$\rho = \text{Max}\{|1 - \omega\lambda| : \lambda \in C\} = \frac{\pi^2/4 - 1}{\pi^2/4 + 1} < 1. \qquad (4.1)$$

Hence we have the same spectral radius as in the case when all eigenvalues are real. Relation (4.1) can easily be shown by recognizing that the maximum is attained on the boundary ∂C. Hence we derive for $\lambda \in \partial C$:

$$\begin{aligned} |1 - \omega\lambda|^2 &= (1 - \omega\rho)^2 + \sigma^2\omega^2 \\ &= 1 - \frac{1}{(1 + \pi^2/4)^2} \\ &\quad \times \left[4\left(1 + \frac{\pi^2}{4}\right)\rho - 4(\rho^2 + \sigma^2) \right] \\ &= 1 - \frac{\pi^2}{(1 + \pi^2/4)^2} = \left(\frac{\pi^2/4 - 1}{\pi^2/4 + 1}\right)^2. \end{aligned}$$

Now we consider the spectral scheme given by (3.4)–(3.7), where the boundary conditions are treated explicitly. The corresponding spectral operator is called L_{sp}^{ex}. FD preconditioning is performed by using the same finite difference approximations as already introduced for the system (3.1)–(3.3). The corresponding FD operator is written as L_{FD}^{ex}. In Figs. 3 and 4 we plotted the eigenvalues of the preconditioned operator $(L_{FD}^{ex})^{-1} L_{sp}^{ex}$ for $N = 8$ and $N = 12$. It is obvious that the imaginary parts are now somewhat larger than for the implicit scheme. They grow for increasing real parts. The (absolutely) maximal eigenvalue has a large imaginary part which also becomes larger for increasing N. In particular, this eigenvalue deteriorates the convergence of an iterative method where the relaxation parameters are based on the interval given by the real parts. Especially, the Richardson iteration with the above relaxation parameter did not converge. Here one has to use some kind of nonsymmetric matrix iterations like GMRES. For the spectral scheme (3.4)–(3.7) we could not find an effective FD pre-

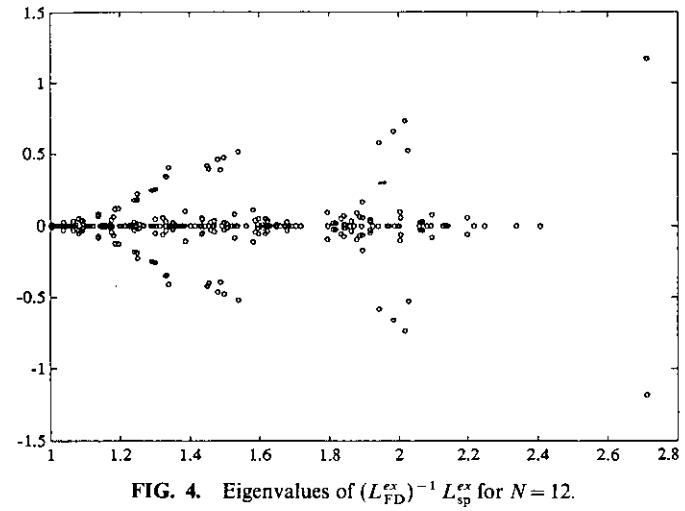

FIG. 4. Eigenvalues of $(L_{FD}^{ex})^{-1} L_{sp}^{ex}$ for $N = 12$.

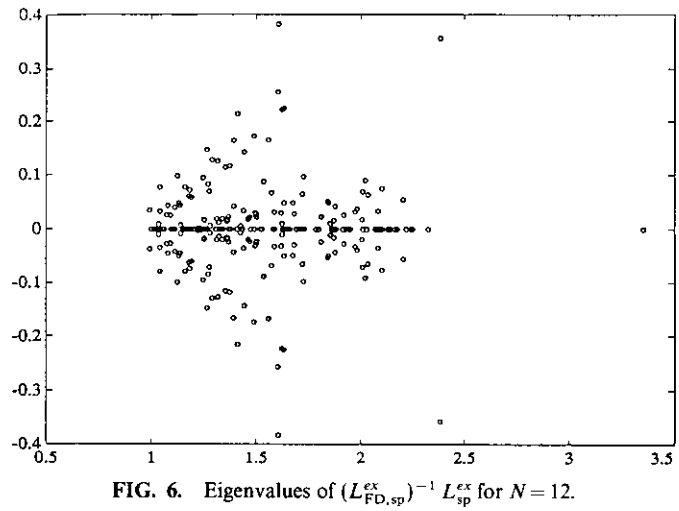

FIG. 6. Eigenvalues of $(L_{FD,sp}^{ex})^{-1} L_{sp}^{ex}$ for $N = 12$.

conditioner. Also higher order FDs could not improve the preconditioning significantly. The problems are caused by the continuity equation (3.7). It results in Neumann boundary conditions for u in $x = \pm 1$ and v in $y = \pm 1$ which lead to a bad performance of preconditioning techniques. In the FD scheme we replaced these conditions by the spectral operators. This modified FD operator is called $L^{ex}_{\mathrm{FD,sp}}$.

In Figs. 5 and 6 we present the eigenspectrum of $(L^{ex}_{\mathrm{FD,sp}})^{-1} L^{ex}_{\mathrm{sp}}$. Now the imaginary parts of the eigenvalues are no more large but the maximal eigenvalue becomes larger for increasing N. However, a disadvantage of the present approach is due to the fact that the continuity equation is now approximated by the spectral scheme which destroys the sparse structure of the FD scheme. Hence in order to construct an effective iterative solver we recommend the implicit treatment of the continuity equation.

Finally we remark that when a variational approach is considered (like in finite elements), the Neumann conditions can easily be incorporated. Then this type of preconditioning is very successful (see [7, 8]).

5. SPECTRAL MULTIGRID METHOD

For a definition of the multigrid method we have to define the relaxation scheme and the grid transfer operators (interpolation and restriction). These multigrid components are used in a multigrid frame (see [3]). This means that we first use a relaxation sweep on the finest grid. Then the resulting residual is restricted to the next coarser grid. Here we once more approximate the coarse grid problem by a relaxation sweep. This procedure is continued until we arrive on the coarsest grid. This problem is solved exactly by a direct solver (for instance, the Gaussian elimination procedure) or by executing a sufficient number of relaxation steps. By means of the interpolation we afterwards correct the approximations up to the finest grid. In the papers of Zang *et al.* [32, 33] the specific spectral multigrid (SMG) components were introduced. Brandt *et al.* [4] have improved them for problems with periodic boundary conditions. Erlebacher *et al.* [9] investigated the specific problems arising from three-dimensional (Fourier-) Helmholtz equations. We achieved in [14, 15] some improvements for the pseudospectral (Chebyshev-) approximation of the Poisson equation with Dirichlet boundary conditions. The experiences made in these investigations are now adopted to the Stokes problem.

For the grid transfers we choose the natural interpolation and restriction operators. The natural interpolation represents interpolation with Chebyshev polynomials with respect to the Chebyshev Gauss–Lobatto nodes. Given a function on a coarse grid, we compute the discrete Chebyshev coefficients and then use the resulting discrete Chebyshev series to construct the interpolated function on the fine grid. This may be accomplished by performing two fast cosinus transforms. The restriction procedure works as follows. Given a function on a fine grid, we compute the discrete Chebyshev coefficients and set those coefficients belonging to the high frequencies to zero. Afterwards we compute the grid function on the coarse grid. If we choose the transfer operators in this natural way they are not adjoint to each other (see also [6, 32, 33]). For a theoretical analysis it is sometimes better to have them adjoint to each other. But by numerical experiments we found no improvements in the convergence rates. Hence we still prefer the above transfer operators.

The most important component of a multigrid method is the relaxation scheme which is responsible for smoothing the high frequencies in the error. Smoothing means that the high frequency components in the error are significantly damped such that a good representation of the error on a coarser grid is guaranted. For SMG methods we recommend a Richardson (or Euler) relaxation with FD preconditioning (or defect correction). Here we consider the spectral scheme (3.1)–(3.3).

If some approximations $\tilde{u}_{N+2,N} \in \mathbf{P}^0_{N+2,N}$, $\tilde{v}_{N,N+2} \in \mathbf{P}^0_{N,N+2}$, $\tilde{p}_N \in \mathbf{P}_N$ (with corresponding defects $\tilde{d}^u_{N+2,N}$, $\tilde{d}^v_{N,N+2}$, $\tilde{d}^p_N$) of the spectral solution are given, the calculation of the new approximation $\bar{u}_{N+2,N}, \bar{v}_{N,N+2}, \bar{p}_N$ proceeds as follows:

1. *Defect computation,*

$$\begin{bmatrix} \bar{d}^u_{N+2,N} \\ \bar{d}^v_{N,N+2} \\ \bar{d}^p_N \end{bmatrix} = \begin{bmatrix} \tilde{d}^u_{N+2,N} \\ \tilde{d}^v_{N,N+2} \\ d^p_N \end{bmatrix} - L_{sp} \begin{bmatrix} \tilde{u}_{N+2,N} \\ \tilde{v}_{N,N+2} \\ \tilde{p}_N \end{bmatrix}.$$

2. *Defect correction.* Compute an approximation

$$\begin{bmatrix} \hat{u}_{N+2,N} \\ \hat{v}_{N,N+2} \\ \hat{p}_N \end{bmatrix}$$

to the exact solution of the FD problem

$$L_{\mathrm{FD}} \begin{bmatrix} \hat{u}_{N+2,N} \\ \hat{v}_{N,N+2} \\ \hat{p}_N \end{bmatrix} = \begin{bmatrix} \bar{d}^u_{N+2,N} \\ \bar{d}^v_{N,N+2} \\ \bar{d}^p_N \end{bmatrix} \tag{5.1}$$

by using a line Gauss–Seidel relaxation.

3. *Richardson step,*

$$\begin{bmatrix} \bar{u}_{N+2,N} \\ \bar{v}_{N,N+2} \\ \bar{p}_N \end{bmatrix} = \begin{bmatrix} \tilde{u}_{N+2,N} \\ \tilde{v}_{N,N+2} \\ \tilde{p}_N \end{bmatrix} - \omega \begin{bmatrix} \hat{u}_{N+2,N} \\ \hat{v}_{N,N+2} \\ \hat{p}_N \end{bmatrix}$$

with a suitable relaxation parameter ω (see Section 4). $\bar{p}_N$ is normalized such that $\int_\Omega \bar{p}_N\, dx = 0$.

The evaluation of the spectral residual (step 1) is the most expensive part of the relaxation procedure. Here we show how it can be accomplished by using fast cosinus transforms which are based on real fast Fourier transforms (FFTs). Since $\tilde{p}_N \in \mathbf{P}_N$ the evaluation of the spectral derivatives $\tilde{p}_{N,x}$, $\tilde{p}_{N,y}$, and $\Delta\tilde{p}_N$ can be accomplished by using the standard technique (see [14]). But it is not immediately clear how to evaluate $\Delta\tilde{u}_{N+2,N}$ (resp. $\Delta\tilde{v}_{N,N+2}$) by FFTs. Clearly, $\tilde{u}_{N+2,N}$, $\tilde{v}_{N,N+2}$ can be written as

$$\tilde{u}_{N+2,N} = (1-x^2)^2\,(1-y^2)\,\tilde{u}_{N-2},$$
$$\tilde{v}_{N,N+2} = (1-x^2)(1-y^2)^2\,\tilde{v}_{N-2},$$

where $\tilde{u}_{N-2}$, $\tilde{v}_{N-2} \in \mathbf{P}_{N-2}$. In order to apply spectral derivative operators we have to determine $\tilde{u}_{N-2}$ (resp. $\tilde{v}_{N-2}$) from the function values of $\tilde{u}_{N+2,N}$ (resp. $\tilde{v}_{N,N+2}$) in $\bar{\Omega}_N$. One straightforward way of accomplishing this goal is by dividing $\tilde{u}_{N+2,N}$ (resp. $\tilde{v}_{N,N+2}$) through $(1-x^2)^2\,(1-y^2)$ (resp. $(1-x^2)(1-y^2)^2$) and then calculating the Chebyshev representation of $\tilde{u}_{N-2}$ (resp. $\tilde{v}_{N-2}$) by using the function values of these functions in Ω_N. However, this approach does not allow the use of FFTs and is quite expensive. It requires a total amount of $O(N^3)$ arithmetic operations.

A more elegant way of determining $\tilde{u}_{N-2}$, $\tilde{v}_{N-2}$ by means of FFTs is described in the following. For simplicity, we consider the one-dimensional case. The problem is that we want to determine the polynomial $\tilde{w}_{N-2} \in \mathbf{P}_{N-2}$ by using the grid values $w_{N+2}(x_i)$, $i = 1, \ldots, N-1$, of the polynomial $w_{N+2} \in \mathbf{P}_{N+2}$ given by

$$w_{N+2} = (1-x^2)^2\,\tilde{w}_{N-2}, \qquad \tilde{w}_{N-2} \in \mathbf{P}_{N-2}.$$

It is immediately seen that

$$\hat{w}_N = \frac{w_{N+2}}{1-x^2} \in \mathbf{P}_N^0.$$

Hence we can calculate the coefficients of its Chebyshev series by using FFTs. Further, we have the identity

$$(1-x^2)\,\tilde{w}_{N-2} = \hat{w}_N.$$

Since both polynomials vanish at the endpoints, it is enough to equate the Chebyshev coefficients of index $\leqslant N-2$ on both sides. The Chebyshev coefficients on the left side can be expressed in terms of a three-term relation. The corresponding tridiagonal matrix is given by $E = (e_{k,l})_{k,l=1,\ldots,N-1}$, where

$$e_{k,l} = \begin{cases} 1 - \frac{1}{4}(c_k + c_{k-1}), & k = l, \\ -\frac{1}{4}c_{k-2}, & k = l+2, \\ -\frac{1}{4}, & k = l-2, \\ 0, & \text{else} \end{cases}$$

and

$$c_k = \begin{cases} 0, & k \leqslant 0, \\ 2, & k = 1, \\ 1, & k \geqslant 2. \end{cases}$$

This representation can for instance be taken from [11, Appendix; or 16]. Hence, in order to determine the Chebyshev coefficients of $\tilde{w}_{N-2}$, we have to solve a tridiagonal system with E which can be accomplished in $O(N)$ arithmetic operations. From numerical experiments we also found that this algorithm is robust with respect to roundoff errors.

In the two-dimensional case we have to solve a system for the matrix

$$E \otimes E = (Ee_{k,l})_{k,l=1,\ldots,N-1} \in \mathbf{R}^{(N-1)^2,(N-1)^2},$$

where $\otimes$ denotes the matrix tensor product. Solving a system with this matrix means solving a tridiagonal system with E twice. Hence the operational account for solving a system related to $E \otimes E$ requires $O(N^2)$ arithmetic operations. From these considerations it becomes clear that also $\Delta\tilde{u}_{N+2,N}$ and $\Delta\tilde{v}_{N,N+2}$ can be evaluated by FFTs which require a total amount of $O(N^2 \ln N)$ arithmetic operations.

For the Richardson step (step 3) we have to define suitable relaxation parameters. In Section 4 we already found that for a stationary Richardson (SR) relaxation the optimal parameter is given by $\omega = 2/(1+\pi^2/4) \cong 0.5768$. The resulting smoothing rate becomes 0.4232. For the nonstationary Richardson (NSR) relaxation the parameters change as the Richardson step changes.

Here we recommend a sweep of three relaxations. The convergence factor results in 0.2797. We further remark that an adaptive parameter choice which, for instance, results from a minimal residual relaxation does not work since—due to the continuity equation—the symmetric part of the preconditioned spectral operator is indefinite (see [6, 5]).

The most interesting part of the relaxation procedure is the defect correction, i.e., the iterative solution of the FD problem (5.1). From our previous work on SMG methods (see [14, 15]) it became clear that line relaxation is necessary in order to obtain sufficient smoothing properties. The Chebyshev grid (which is dense near the boundary) introduces locally different anisotropies. This can only be smoothed by a line relaxation technique. Here we propose

an (alternating) zebra line Gauss–Seidel relaxation. Now we describe the defect correction in more detail.

First of all we express the boundary values of p_N by using function values of $u_{N+2,M}$ (resp. $v_{N,N+2}$ and p_N) in points next to the boundary. Here we make use of the collocation equations in the boundary points of Ω_N^u (resp. Ω_N^v). For this purpose we introduce the step size

$$h_1 = 1 - \cos\frac{\pi}{N} = 2\sin^2\frac{\pi}{2N}$$

and points $x_1 = \cos(\pi/N)$, $x_{N-1} = \cos((N-1)\pi/N)$. The collocation conditions in $x = \pm 1$ are given by

$$\frac{2}{h_1^2}(u_{N+2,N}(1, y_j) - u_{N+2,N}(x_1, y_j)) + \frac{1}{h_1}(p_N(1, y_j) - p_N(x_1, y_j)) = \bar{d}^u_{N+2,N}(1, y_j), \qquad j = 1, \ldots, N-1,$$

and

$$\frac{2}{h_1^2}(u_{N+2,N}(-1, y_j) - u_{N+2,N}(x_{N-1}, y_j)) - \frac{1}{h_1}(p_N(-1, y_j) - p_N(x_{N-1}, y_j)) = \bar{d}^u_{N+2,N}(-1, y_j), \qquad j = 1, \ldots, N-1.$$

Hence we obtain by using $u_{N+2,N}(1, y_j) = 0$,

$$p_N(1, y_j) = h_1 \bar{d}^u_{N+2,N}(1, y_j) + \frac{2}{h_1} u_{N+2,N}(x_1, y_j) + p_N(x_1, y_j), \qquad j = 1, \ldots, N-1,$$

and a similar equation for $p_N(-1, y_j)$.

A similar expression for p_N can be derived in $y = \pm 1$ by using the collocation conditions in the boundary points of Ω_N^v. Hence the boundary values of p_N in $y = \pm 1$ can be expressed by values of $v_{N,N+2}$ and p_N in points next to the boundary. Furthermore, by using the collocation conditions in the four corners, we can determine the values of p_N in the corner points. For instance, in $(x, y) = (1, 1)$ we obtain

$$p_N(1, 1) = p_N(x_1, 1) + h_1 \bar{d}^u_{N+2,N}(1, 1),$$

where $p_N(x_1, 1)$ can be expressed by values of $v_{N,N+2}$, p_N in the point $(x_1, x_1) \in \Omega_N$. Hence we have eliminated all function values in boundary points and we can write the FD system for unknowns $u_{N+2,N}$, $v_{N,N+2}$, p_N defined in Ω_N. These are

$$\tilde{M} = 9(N-1)^2$$

unknowns which are determined by the $\tilde{M}$ conditions of collocation in the points of Ω_N. Afterwards the boundary values are updated by using the above relations in boundary points. Now our $\tilde{M} \times \tilde{M}$-system is approximately solved by one or two steps of a line Gauss–Seidel relaxation. Here one first relaxes along lines of constant x and afterwards along lines of constant y. Vectorization is achieved by first solving for the odd lines and then for the even lines, resulting in zebra line relaxation. A more precise description is given in [4, 14].

Now we examine the structure of the matrices of the Gauss–Seidel relaxation relative to a fixed line, here for fixed $y = y_j$. The Laplace operator introduces three nonvanishing diagonals and p_x introduces two nonvanishing diagonals. Furthermore the collocation conditions in points next to the boundary relative to p_x and Δp introduce values of $u_{N+2,N}$ in points next to the boundary. Hence we finally obtain a $3(N-1) \times 3(N-1)$ system with seven nonvanishing diagonals. We plotted the structure of these matrices in Fig. 7. The non-zero entries are marked by a ★. Since a Gaussian elimination procedure applied to this type of matrix would fill up the matrix and destroy the sparse structure we recommend a renumbering of the grid points. If we fix $j \in \{1, \ldots, N-1\}$ the above matrix is applied to the vector

$$[u_{1,j}, \ldots, u_{N-1,j}, v_{1,j}, \ldots, v_{N-1,j}, p_{1,j}, \ldots, p_{N-1,j}]^t,$$

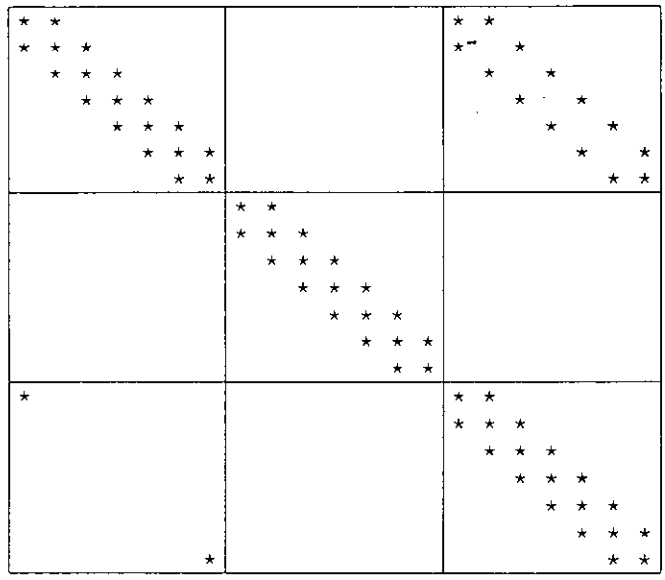

FIG. 7. Structure of submatrices for Gauss–Seidel line relaxation ($N = 8$).

where we write: $u_{i,j}=u_{N+2,N}(x_i, y_j)$, $v_{i,j}=v_{N,N+2}(x_i, y_j)$, $p_{i,j}=p_N(x_i, y_j)$. Now we renumber the components of this vector in the following way

$$[p_{1,j}, v_{1,j}, u_{1,j}, p_{2,j}, v_{2,j}, u_{2,j}, \ldots, p_{N-1,j}, v_{N-1,j}, u_{N-1,j}]^t.$$

After a corresponding renumbering in the matrix we obtain a modified $3(N-1)\times 3(N-1)$ matrix with seven nonvanishing diagonals (main diagonal, first, second, and third diagonals besides the main diagonal). For this type of matrix the Gaussian elimination procedure can be performed very efficiently. There is no fillup of the zero diagonals and hence the computational amount of work for solving these systems is proportional to N. Hence one complete sweep of the line Gauss–Seidel method requires $O(N^2)$ arithmetic operations. For a more detailed description of the line Gauss–Seidel relaxation we refer to [4, 14].

6. NUMERICAL RESULTS

In the numerical computations we generally use a V-cycle with two ($N=4, 8$), three ($N=4, 8, 16$), or four ($N=4, 8, 16, 32$) grids. In order to measure the convergence speed of the (SMG) method we calculated the spectral radius ρ of the SMG operator by means of the power method. A convergence factor which is related to the computational work can be defined by $\rho_W=\rho^{1/W}$, where $W=n_d+n_u$ and n_d (resp. n_u) denote the number of relaxations on each grid in the downward (resp. upward) branches, respectively. ρ_W does not take the total computational work into account but it should be near the smoothing rate and provide an estimate of efficiency. From numerical experiments we found that the number of relaxations should be

$$n_d=n_u=3 \qquad \text{for the SR and NSR relaxation}$$

and the number of preconditioning (PC) steps should be two. In Table II we present the spectral radius of the corresponding Richardson relaxation without using multigrid techniques. In Table III we give the results for the SMG method.

The numerical results substantiate the usefulness of SMG compared to the Richardson iteration. Furthermore, it shows the improvements by choosing two PC steps of the Gauss–Seidel line relaxation. One PC step is not enough for a good smoothing of the high frequencies. If we employ two steps the convergence rates are quite similar to the rates we already observed for the Poisson equation (see [14]). Similar results were also obtained by other cycle structures. For instance, the W-cycle could not improve the convergence factors. The rates were nearly the same as for the V-cycle.

TABLE II

ρ_W for the Richardson Iteration

N	1 PC step	2 PC steps
8	0.5670	0.6891
16	0.8435	0.9172
32	0.9640	0.9691

TABLE III

ρ_W for the SMG Method

Number of grids	Relaxation	1 PC step	2 PC steps
2	SR	0.5834	0.4346
2	NSR	0.5286	0.4000
3	SR	0.6223	0.4641
3	NSR	0.5420	0.4269
4	SR	0.7104	0.4769
4	NSR	0.5415	0.4440

Finally, we solved a driven cavity flow problem given by

$$f^u=0, \qquad f^u=0,$$

$$u_0(x, y)=\begin{cases}0 & \text{if } y<1,\\ (1-x^2)^2 & \text{if } y=1,\end{cases} \qquad v_0(x, y)=0.$$

We once more considered the spectral scheme (3.1)–(3.3). Especially, the continuity equation $u_x+v_y=0$ appears only as a boundary condition in the reformulated system. This has the consequence that its discrete analogue does not hold exactly but only up to some error caused by the discretization. Hence we calculated the discrete L^2-norm $D2$ and maximum norm DM of $z_N=(u_{N+2,N})_x+(v_{N,N+2})_y$ in $\bar{\Omega}_N$. We explicitly define

$$D2=\frac{1}{\sqrt{N}}\sqrt{\sum_{i,j=0}^{N} z_N^2(x_i, y_j)},$$

$$DM=\operatorname{Max}\{|z_N(x_i, y_j)|:(x_i, y_j)\in\bar{\Omega}_N\}.$$

In Table IV we present $D2$, DM for $N=8, 16, 32$. The results are compared to the corresponding results $D2_{\mathrm{FD}}$, DM_{FD} of the finite difference method [31]. We observe the

TABLE IV

Results for the Driven Cavity Flow Problem

N	$D2$	DM	$D2_{\mathrm{FD}}$	DM_{FD}
8	6.8624×10^{-4}	9.3903×10^{-3}	8.1×10^{-2}	3.6×10^{-1}
16	3.3312×10^{-6}	4.3427×10^{-4}	2.2×10^{-2}	1.2×10^{-1}
32	7.0570×10^{-7}	1.3241×10^{-4}	5.7×10^{-3}	3.2×10^{-2}

high accuracy of the spectral methods. We further remark that in any case four V-cycles are enough to reach this accuracy.

We also tried to solve the corresponding Navier–Stokes equations. But due to the occurrence of first-order derivatives the preconditioning fails also for low Reynolds numbers. The real parts of the eigenvalues are close to zero. Hence also SMG methods yield bad convergence properties. In order to obtain a good preconditioner one has to introduce a staggered grid preconditioning (see [6, Chap. 5.2.2; 10]). Then the real parts of the eigenvalues are safely bounded greater than zero. Unfortunately, this preconditioner is not suitable for SMG methods since it yields a dense matrix.

Recently we had good experience with upstream preconditioning, where the first derivatives are approximated by one-sided finite differences. Here the first derivatives are differenced according to the sign of the preceding coefficients. The discretization is performed in such a way that the resulting matrix becomes diagonally dominant. For the iterative solution we recommend flow directed schemes. We once more use line Gauss–Seidel relaxation for smoothing. It is recommended to use alternate iterations of FDHI (flow directed horizontal iterations) and FDVI (flow directed vertical iterations). This iterative procedure is called FDHVI (see [12]). Preconditioning by FDHVI introduces a spectrum of eigenvalues which are complex with relatively large imaginary parts. Hence for the iterative solution we recommend some nonsymmetric matrix iteration. In particular, we recommend the GMRES iteration (see [26, 29, 30]) which belongs to the residual minimization methods. Then also for time-dependent flows it is possible to use an implicit treatment of the nonlinear terms. There are many important applications, where the accuracy limitations make an explicit treatment of the nonlinear terms sensible.

For three-dimensional flows we recommend the use of (alternating) plane relaxation techniques. The plane relaxation requires the solution of 2D finite difference problems which are solved approximately by using 2D multigrid cycles. For elliptic model problems in 3D we have shown the efficiency of this smoothing procedure in [17].

REFERENCES

1. C. Bernardi, C. Canuto, and Y. Maday, *SIAM J. Numer. Anal.* **25**, 1237 (1988).
2. C. Bernardi, and Y. Maday, *Int. J. Numer. Methods Fluids* **8**, 537 (1988).
3. A. Brandt, in *Proceedings, Conference held at Köln-Porz, Germany, 1981*, edited by A. Dold and B. Eckmann (Springer-Verlag, New York, 1982).
4. A. Brandt, S. R. Fulton, and G. D. Taylor, *J. Comput. Phys.* **58**, 96 (1985).
5. C. Canuto, *SIAM J. Numer. Anal.* **23**, 815 (1986).
6. C. Canuto, M. Y. Hussaini, A. Quarteroni, and T. A. Zang, *Spectral Methods in Fluid Dynamics*, 1st ed., Series in Computational Physics (Springer-Verlag, Berlin/Heidelberg/New York, 1989).
7. C. Canuto and P. Pietra, *J. Comput. Phys.* **105** (1993).
8. M. Deville and E. Mund, *J. Comput. Phys.* **60**, 517 (1985).
9. G. Erlebacher, T. A. Zang, and M. Y. Hussaini, in *Multigrid Methods*, edited by S. McCormick and K. Stüben (Marcel Dekker, New York, 1987).
10. D. Funaro, *SIAM J. Numer. Anal.* **24**, 1024 (1987).
11. D. Gottlieb and S. A. Orszag, *Numerical Analysis of Spectral Methods: Theory and Applications* (SIAM-CBMS, Philadelphia, 1977).
12. H. Han, V. P. Il'in, and R. B. Kellogg, in *BAIL V, Proceedings, Fifth Int. Conf. on Boundary and Interior Layers—Computational and Asymptotic Methods*, edited by G. Ben-yu, J. J. H. Miller, and S. Zhong-ci (Shanghai, China, 1988).
13. F. H. Harlow and J. E. Welch, *Phys. Fluids* **8**, 2182 (1965).
14. W. Heinrichs, *J. Comput. Phys.* **77**, 166 (1988).
15. W. Heinrichs, *J. Comput. Phys.* **78**, 424 (1988).
16. W. Heinrichs, *Math. Comput.* **53**, 103 (1989).
17. W. Heinrichs, *Appl. Math. Comput.* **41**, 117 (1991).
18. W. Heinrichs, *J. Comput. Phys.* **102**, 310 (1992).
19. W. Heinrichs, *SIAM Sci. Statist. Comput.*, submitted.
20. W. Heinrichs, *Appl. Math. Comput.* to appear.
21. W. Heinrichs, "Finite Element versus Finite Difference Preconditioning for Spectral Multigrid Methods," Proceedings, IMACS International Symposium on Iterative Methods in Linear Algebra, Brussels, 1991.
22. C. W. Hirt and F. H. Harlow, *J. Comput. Phys.* **2**, 114 (1967).
23. L. Kleiser and U. Schumann, in *Spectral Methods for Partial Differential Equations*, edited by R. G. Voigt, D. Gottlieb, and M. Y. Hussaini (SIAM, Philadelphia, 1984).
24. J. Linden, G. Lonsdale, B. Steckel, and K. Stüben, Arbeitspapiere der GMD 294, Gesellschaft für Mathematik und Datenverarbeitung, St. Augustin, 1988 (unpublished).
25. J. Linden, B. Steckel, and K. Stüben, Arbeitspapiere der GMD 322, Gesellschaft für Mathematik und Datenverarbeitung, St. Augustin, 1988 (unpublished).
26. N. M. Nachtigal, S. C. Reddy, and L. N. Trefethen, Numerical Analysis Report 90-2, Department of Mathematics, MIT, 1990 (unpublished).
27. P. J. Roache, *Computational Fluid Dynamical* (Hermosa, Albuquerque, NM, 1976).
28. E. Ronquist, PhD. thesis, MIT, 1988.
29. Y. Saad and M. H. Schultz, *Math. Comput.* **44**, 417 (1985).
30. Y. Saad and M. H. Schultz, *SIAM J. Sci. Statist. Comput.* **7**, 856 (1986).
31. A. Schüller, in *Numerical Treatment of the Navier–Stokes Equations, Proceedings, Fifth GAMM-Seminar*, edited by W. Hackbusch and R. Rannacher (Vieweg, Braunschweig, 1990).
32. T. A. Zang, Y. S. Wong, and M. Y. Hussaini, *J. Comput. Phys.* **48**, 485 (1982).
33. T. A. Zang, Y. S. Wong, and M. Y. Hussaini, *J. Comput. Phys.* **54**, 489 (1984).